New Method for Magnet Protection Systems Based on a Direct Current Derivative Sensor

E. De Matteis, D. Calcoen, R. Denz, A. Siemko, J. Steckert, and M. B. Storkensen

***Abstract*—A new method of the quench detection systems (QDS) designed for the LHC 600 A corrector magnet circuits and 6 kA individual powered quadrupole (IPQ) magnet circuits is presented. In order to improve the dependability of QDS, a direct measurement of the current derivative is proposed. The quench detection scheme for the 600 A corrector magnet circuits uses the current derivative numerically evaluated from a direct current measurement. In order to make the calculation stable, the current derivative is heavily filtered, thus introducing a significant phase shift, which restricts the operational range of circuit parameters such as the acceleration. For the 6-kA IPQ magnet circuits the main quench detection is based on a classical bridge configuration. The introduction of an additional detection channel for the direct measurement of the current derivative helps to overcome the lack of sensitivity to fully aperture symmetric quenches of the bridge configuration. Transformer-based current derivative sensors are currently under development, using cut cores for easy prototyping, performance control, and installation. Prototypes for the ±600 A current range and ramp rates between 0.1 and 5 A/s were built using different core materials (electrical steel and nanocrystalline cores) and pickup coils with 10 000 and 20 000 windings. In order to characterize the prototypes, the performance was defined in terms of mean sensitivity of the sensor response in [V/A/s] and the performance quality factor (PQF), defined as a percentage of nonlinearity of the response. An optimization procedure was implemented for finding the best configuration of the sensors, i.e., the air gap in the cut core in order to maximize the mean sensitivity and to minimize the PQF. The tests were carried out at different working points (current ranges and ramp rates) showing promising results (PQF $<0.5\%$ with a sensitivity of 5.5 mV/A/s).**

***Index Terms*—Control equipment, protection, current measurement, sensor, transformer cores, superconducting magnets.**

I. Introduction

THE quench protection system of the LHC is a fundamental part of the machine in order to protect the superconducting magnets. Apart from the presence of passive protection elements, *i.e.,* cold by-pass diodes and cold parallel extraction resistors, the quench detection system coordinates and triggers the operation of the active protection elements as the quench heater discharge power supplies and energy extraction systems [1]–[3]. The superconducting circuits supervised by the active protection have different protection configurations, depending on the circuit layout and the number and type of superconducting elements. The protected circuits have nominal current ratings from 550 A to 11870 A [4], [5].

Manuscript received August 25, 2017; accepted January 13, 2018. Date of publication January 23, 2018; date of current version February 2, 2018. *(Corresponding author: E. De Matteis.)*

The authors are with the Machine Protection and Electrical Integrity Group, Technology Department, CERN, Geneva CH-1211, Switzerland (e-mail: ernesto.de.matteis@cern.ch).

Color versions of one or more of the figures in this paper are available online at http://ieeexplore.ieee.org.

Digital Object Identifier 10.1109/TASC.2018.2795553

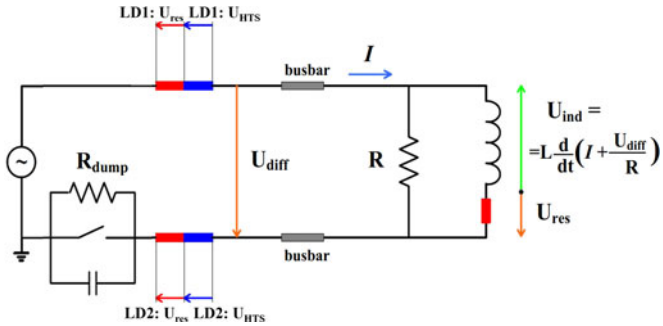

Fig. 1. Protection circuit for 600 A corrector magnets.

The quench protection for the 600 A corrector magnet circuits of the LHC combines the magnet and circuit protection and determines the resistive voltage with the help of a complex numerical calculation described below, see also [6]. Hereby the numerical determination of the current derivative is crucial but introduces systematic errors limiting the range of operational parameters like the acceleration of the magnet current ramp rate. The proposed method based on the direct current derivative measurement could represent a solution for this problem and ease the operation of these circuits. The 6 kA IPQ magnet protection could benefit from the direct current derivative measurement as a complementary method exploiting its sensitivity to aperture symmetric quenches, which are difficult to detect with detection systems operating in the classical bridge configuration.

II. Quench Detection Systems for 600 A Corrector Magnet Circuits

Depending on the stored energy and magnet type the quench protection for this type of circuits is provided by the power converter crow bar, external energy extraction systems and/or cold parallel resistors [6], [7]. A typical example is shown in Fig. 1. In case of a quench, the detection system will stop the power converter and activate the energy extraction system thus allowing the energy stored in the circuit to be safely dissipated. The quench detection system uses the voltage drop across the cold part of the circuit U_{diff} and the current I measured by a Hall sensor [8] as input signals and determines the resistive voltage U_{res} with the help of numerical algorithm based on the

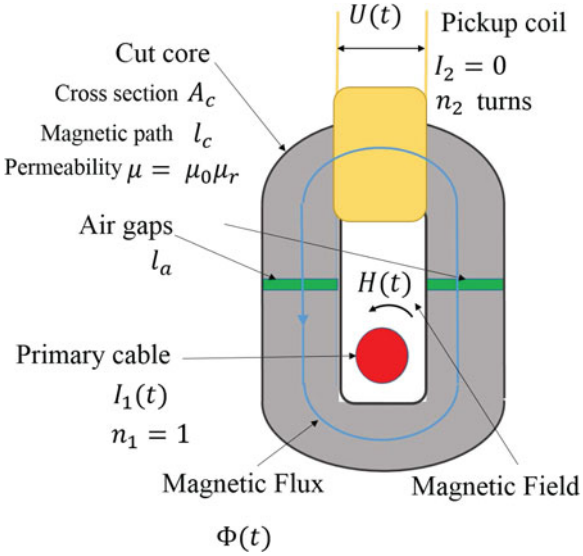

Fig. 2. Transformer-based sensor model.

following formula:

$$U_{res} = U_{diff} + L(I)\frac{d}{dt}\left(I + \frac{U_{diff}}{R}\right) \tag{1}$$

The circuit inductance as a function of the current has been determined empirically for each individual circuit type and is stored as a look-up table in the device memory. The numerical determination of the current derivative requires digital filtering, which introduces a phase shift with respect to the U_{diff} signal resulting in an apparent resistive voltage during acceleration. While this does not affect the protection functionality, it is disadvantageous for the accelerator operation by limiting the maximum speed which the circuit can be ramped. The current algorithm limits the power converter acceleration to maximum 1 A/s^2 and, consequently, the ramp rates to 5 A/s [4]. This limitation could result critical for the future orbital correction needs required by the new beam optics for the High Luminosity − LHC upgrade.

III. Proposed Method

The use of the direct current derivative measurement could be exploited in two different LHC quench detection systems namely the protection of 600 A corrector magnet circuits and the IPQ magnet circuits. The application for the 600 A circuits requires the development of a sensor with a fine resolution of 0.05 A/s in the range of $\pm(0.1 \div 5)$ A/s [4], [5], while the improved protection of the insertion region magnets calls for the detection of fast ramp rates $\pm(50 \div 200)$ A/s with a coarse resolution of about 0.5 A/s. Both specifications are not covered by commercially available devices.

A. Direct Current Derivative Sensor

The technology selected for implementing the direct current derivative measurement is the transformer-based one [9], [10]. The proposed technology shows various advantages. The design has limited complexity and hence eases prototyping (see Fig. 3).

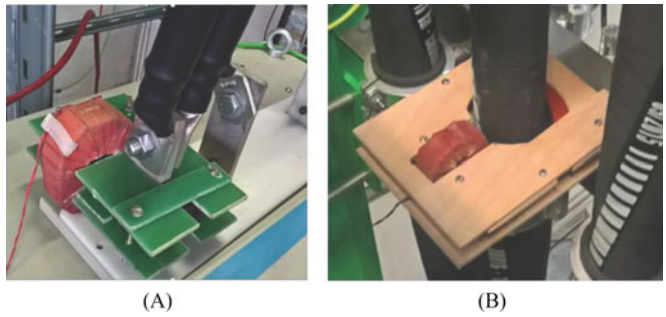

Fig. 3. Current derivative sensor prototypes: (A) 600 A nanocrystalline core based sensor integrated on top of an energy extraction system (130 × 76 × 26 mm) with a 20000 windings coil and (B) 6 kA sensor prototype based on a nanocrystalline core installed on a 3 kA cable.

Using a cut core configuration, the performance optimization is relatively easy by adjusting the air-gap. The installation of the sensor does not require a modification of the existing circuit nor a cutting of the power cables. Last but not least, the passive nature of the sensor could improve significantly the reliability of the signal. In the following subsections, the magnetic circuit model and the prototyping of the above-mentioned sensor are detailed.

1) Magnetic Circuit Model: The sensor model was mainly based on the power transformer principle [9]. By applying Faraday's law to the sensor model shown in Fig. 2, the magnetic flux variation inside the core induces a voltage:

$$U(t) = n_2\frac{d\Phi(t)}{dt} \tag{2}$$

From Ampère's law, the total current passing through the magnetic path l_c (see Fig. 2) is equal to the magnetomotive force F_c (MMF) of the core, for an uniform field strength $H(t)$:

$$F_c = H(t)l_c = n_1 I_1(t) = I_1(t) \tag{3}$$

The magnetic field $H(t)$ as a function of the magnetic flux $\Phi(t)$:

$$H(t) = \frac{\Phi(t)}{A_c\mu} \tag{4}$$

Applying the Kirchhoff's magnetic law $F = R\Phi$ to the relative magnetic circuit [9], the final model gives:

$$U(t) = \frac{\mu A_c n_2}{l_c + 2\mu_r l_a}\frac{dI_1(t)}{dt} \tag{5}$$

The current rate of the sensor is established by the saturation current of the core, which is a function of the saturation field:

$$I_{sat} = \frac{B_{sat}A_c}{n_1}(R_c + R_a) \tag{6}$$

where R_c and R_a are the core and air-gap reluctances, and B_{sat} is the saturation field of the core material.

2) Prototyping: The prototypes were based on the cut-core transformer (see Fig. 3). The first prototyping phase was focused on the choice of the best core material. Two core materials have been tested: electrical steel, or lamination steel (relative permeability of about 4000 and saturation field B_{sat} of 0.3 T), used in the classical power transformers, and a nanocrystalline material

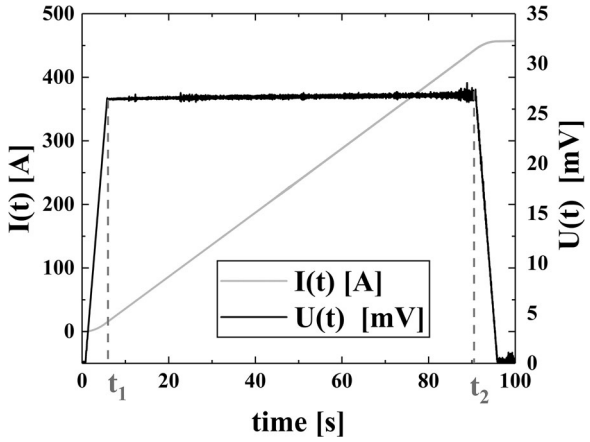

Fig. 4. Sensor voltage (black) recording during a current ramp (gray line). Start and stop points (t_1 and t_2) for the calculation of the mean value are highlighted.

made of Vitroperm500 (relative permeability of about 50000 and saturation field B_{sat} of 1.2 T) [11]. The air-gap between the two cut cores, and the number of pickup coil windings, 10000 and 20000, represented the two tuning parameters of the sensor. As shown in (6), increasing the air-gap decreases the effect of the core magnetization and the core saturation current increases, *i.e.*, the sensor range. After having established the material and the configuration (air-gap and coil) of the sensor, tow prototype devices for the 600 A and 6 kA magnets were realized [see Fig. 3(A) and (B)]. The sensors were assembled in a sandwich-like system in order to tighten the two cut cores.

B. Performance Definitions

The qualification of the sensors focuses on two parameters: the mean sensitivity and a numerical Performance Quality Factor (PQF). The mean sensitivity is a definition of the strength of the sensors response to the ramp rate, measured in volts per amps per second. The PQF is based on the standard deviation and the mean value of the di/dt during linear ramps (see Fig. 4). The mean value of the sensor voltage during ramp would be the ideal response. It is used in the calculation of both mean sensitivity and PQF:

$$U_{mean} = \frac{1}{t_2 - t_1} \int_{t_1}^{t_2} U(t)dt \text{ [V]} \tag{7}$$

The mean sensitivity is calculated from the mean voltage:

$$S_{mean} = \frac{U_{mean}}{\frac{dI}{dt}} \left[\frac{\text{V}}{\frac{\text{A}}{\text{s}}}\right] \tag{8}$$

To enumerate the PQF, the standard deviation has to be calculated:

$$\sigma_{(t_1,t_2)} = \sqrt{\frac{1}{N-1} \sum_{i=1}^{N} (U_i - U_{mean})^2} \text{ [V]} \tag{9}$$

The PQF is defined as:

$$PQF = \frac{\sigma}{U_{mean}} * 100 \text{ [\%]} \tag{10}$$

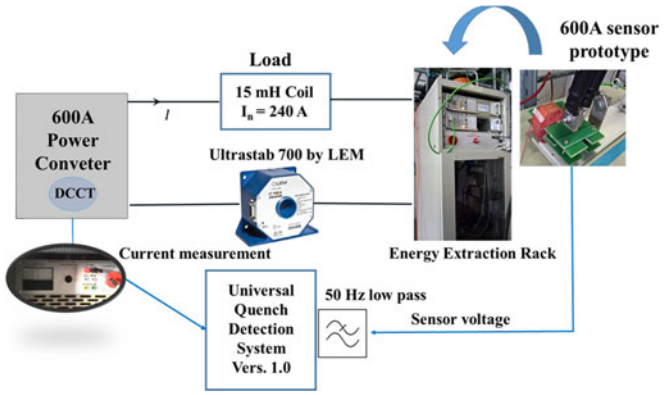

Fig. 5. 600 A sensor measurement setup consisting of a 600 A–10 V power converter connected in series with a coil of 15 mH (emulating a magnet) and a 600 A energy extraction system [7]. The didt sensor [integrated version, Fig. 3(A)] is installed on top of the energy extraction system. The current sensor (LEM transducer [13]) signal and the sensor voltage were acquired with the help of custom made digital quench detection system (three channels with 20 bit SAR ADC, 100 kHz bandwidth and ±21 V input voltage range) [12].

TABLE I
RESULTS OF THE OPTIMIZATION PROCEDURE FOR THE VITROPERM 500 BASED 600 A SENSOR PROTOTYPE FOR DIFFERENT AIR-GAPS AND A FIXED PICKUP COIL (10000 WINDINGS)

Airgap mm	PQF %	σ mV	S_{mean} mV/A/s	I_{sat} A
0.6	1.53	0.919	11.92	580
1.3	0.45	0.142	6.31	1250
1.6	0.44	0.118	5.31	1530
2.0	0.75	0.169	4.47	1910
2.6	0.56	0.102	3.62	2480

The measurements were performed within a current range (0 – 400) A with ramp rate of 5 A/s and an acceleration of 1 A/s^2

The standard deviation considers the core magnetization process (drift of voltage level) and noise effects in the signal. A smaller PQF can mean both: better linearity and less noise sensitivity.

IV. FEASIBILITY TESTS

The two main objectives of the test campaign were the determination of the sensor characteristics (core material, coils) and the proof of principle for the direct measurement of the current derivative at different ramp rates. Regarding the 600 A sensor prototypes the measurement set-up is shown in Fig. 5. The first tests for the determination of the sensor characteristics were performed with two different core materials. The Vitroperm500 based prototype has shown the best performance in terms of PQF ($PQF < 0.5\%$) compared to the one made of electrical steel (PQF of about 2.0%). In order to identify the best configuration of the sensor, an optimization procedure was established measuring the performance for different air-gap values. The results of these measurements, which are reported in Table I, show that the best performance of the sensor is achieved for an air-gap of about 1.5–1.6 mm. The second series of tests concerned the functional aspects of the sensor such as the verification of

TABLE II
CHARACTERIZATION TESTS FOR DIFFERENT MAGNET WORKING POINTS (A/s, A/s^2) OF THE 600 A DIDT INTEGRATED SENSOR (SEE FIG. 5) WITH AN AIR-GAP OF 1.5 mm AND A SATURATION CURRENT OF $I_{sat} = 1.5$ kA

Ramp rate A/s	Acc. A/s^2	Range A	PQF %	σ mV	S_{mean} mV/A/s
5.0	1.0	0–200	0.15	0.05	5.02
3.0	1.0	0–200	0.40	0.05	5.02
1.5	0.1	0–200	0.55	0.04	5.02
0.3	0.1	0–200	0.92	0.02	5.02

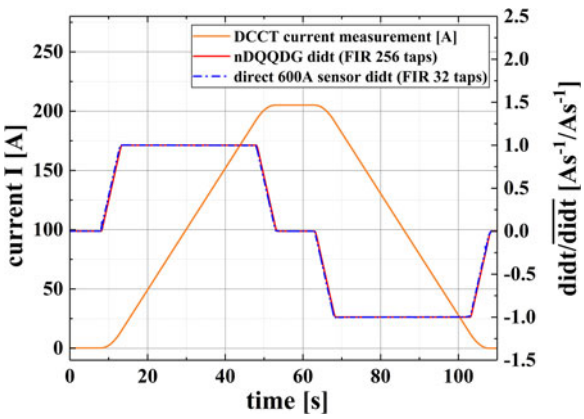

Fig. 6. Test run up to 200 A with 5 A/s and 1 A/s^2 comparing the relative didt measurement made by the 600 A integrated didt sensor prototype and the nDQQDG quench detection system [6].

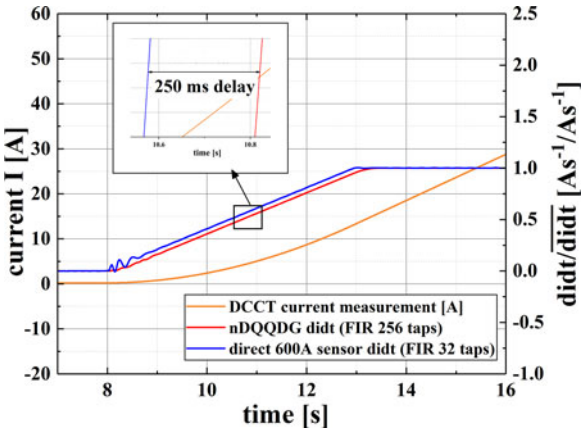

Fig. 7. Phase shift comparison between the nDQQDG quench detection system [6] and the 600 A integrated didt sensor prototype.

the performance in one of the possible final configurations for installation [see Fig. 3(A)]. The copper bus-bars connecting the energy extraction system (see Fig. 5) to the circuit could be one of the less invasive positions for installing the sensor. The results of the characterization tests for the Vitroperm500 based integrated sensor [see Fig. 3(A)] are reported in Table II. The results highlight a PQF less than 1% in general, and less/or equal to 0.5% for the majority of the magnet working points (5.0–1.5 A/s and 1.0–0.1 A/s^2).

The Figs. 6 and 7 show the comparison between the direct didt measurement of the integrated 600 A sensor and the numerical didt measured by the nDQQDG [6] type digital quench detection system used for the protection of the LHC 600 A corrector magnet circuits. As shown in Fig. 7 the new sensor type does not present any phase shift during current acceleration. The noise level of the sensor at a constant current ramp rate is in the order of a few ‰ (Table II, PQF $< 1\%$), which is fully acceptable for operation.

TABLE III
CHARACTERIZATION TESTS FOR DIFFERENT MAGNET WORKING POINTS (A/s, A/s^2) OF THE 6 kA DIDT INTEGRATED SENSOR [SEE FIG. 3(B)] WITH AN AIR-GAP OF 3.0 mm AND A SATURATION CURRENT $I_{sat} = 2.8$ kA

Ramp rate A/s	Acc. A/s^2	Range A	U_{meas} mV	U_{mod} mV	S_{mean} mV/A/s
5.0	1.0	0–200	6.18	6.00	1.28
3.0	1.0	0–200	3.84	3.60	1.28
1.5	0.1	0–200	1.93	1.80	1.28

Regarding the 6 kA sensor prototype, shown in Fig. 3(B) a characterization campaign was done so far only with currents up to 200 A. The results presented in Table III compare the measurement performance with the prediction of the model [see (8) and (5)].

V. CONCLUSION

The paper presents a new method for the quench detection in superconducting magnet circuits based on a novel direct current derivative sensor. Possible applications of the new method are the quench detection systems for the 600 A corrector magnet circuits of the LHC and the protection of the IPQ magnets, especially the timely detection of aperture symmetric quenches. The research and development performed so far concluded in the construction of several prototype devices, which have been submitted to an extensive type test campaign. The outcome of these tests confirmed the validity of the selected technology and its potential to improve the performance of the present generation of quench detection systems used in the LHC. The future activities will regard the possibility of improving the electromagnetic shielding of the sensors in order to decrease the noise and the environmental effects. It is also foreseen to realize field tests with both prototypes (600 A and 6 kA sensors). Preliminary tests with the 6 kA sensor prototype demonstrate the feasibility of the approach but must be complimented by tests with real magnets to validate its functionality as a quench detection system.

ACKNOWLEDGMENT

The authors would like to thank F. Boisier, G. Fodi, V. Froidbise, S. Georgakakis, and J. Spasic from the TE-MPE-EP section and G.-J. Coelingh and B. Panev from the TE-MPE-EE section for their technical and professional help.

REFERENCES

[1] K. Dahlerup-Petersen *et al.*, "The protection system for the superconducting elements of the Large Hadron Collider at CERN," in *Proc. Particle Accel. Conf.*, 1999, vol. 5, pp. 3200–3202.

[2] K. Dahlerup-Petersen, R. Denz, D. Milani, F. Rodriguez-Mateos, and F. Tegenfeldt, "The quench protection system for the LHC test string 2," *IEEE Trans. Appl. Supercond.*, vol. 14, no. 2, pp. 251–254, Jun. 2004.

[3] Z. Charifoulline *et al.*, "Overview of the performance of quench heaters for high-current LHC superconducting magnets," *IEEE Trans. Appl. Supercond.*, vol. 27, no. 4, Jun. 2017, Art. no. 4700405.

[4] M. Pojer and M. Solfaroli Camillocci, "Parameters for LHC superconducting circuits powering tests," CERN, Geneva, Switzerland, CERN Rep., LHC-MPP-HCP-0103, 2016.

[5] R. Denz, "Electronic systems for the protection of superconducting elements in the LHC," *IEEE Trans. Appl. Supercond.*, vol. 16, no. 2, pp. 1725–1728, Jun. 2006.

[6] J. Steckert and A. Skoczen, "Design of FPGA-based radiation tolerant quench detectors for LHC," *J. Instrum.*, vol. 12, 2017, Art. no. T04005.

[7] G. J. Coelingh *et al.*, "Design and commissioning of the energy extraction systems for the LHC corrector magnet circuits," in *Proc. IEEE Int. Power Modulators High Voltage Conf.*, 2008, pp. 465–468.

[8] LEM, "Current transducer HASS 600-S," 2014. [Online]. Available: http://www.lem.com/docs/products/has_50_600-s_e.pdf

[9] R. W. Erickson and D. Maksimovic, "Basic magnetics theory," in *Fundamentals of Power Electronics*. Berlin, Germany: Springer, 2007, ch. 13.

[10] T. M. Wolbank, J. L. Machl, and H. Hauser, "Derivative current sensor for inverter fed ac machines," *Sens. Actuators A, Phys.*, vol. 106, pp. 126–129, 2003.

[11] VAC Vacuumschmelze, "Nanocrystalline cut cores made of vitroperm 500 for transformers," 2016. [Online]. Available: http://www.vacuumschmelze.com/en/products/cores-components/applications/cores/nanocrystalline-cut-cores-made-of-vitroperm-500-for-power-transformers.html

[12] R. Denz, E. De Matteis, A. Siemko, and J. Steckert, "Next generation of quench detection systems for the high-luminosity upgrade of the LHC," *IEEE Trans. Appl. Supercond.*, vol. 27, no. 4, Jun. 2017, Art. no. 4700204.

[13] LEM, "ITN 600-S ULTRASTAB," 2014. [Online]. Available: http://www.lem.com/hq/en/component/option,com_catalog/task,displaymodel/id,71.44.52.000.0/